POLITECNICO DI TORINO
Repository ISTITUZIONALE

New Resilience Index for Urban Water Distribution Networks

(Article begins on next page)

16 January 2025

1   **A NEW RESILIENCE INDEX FOR URBAN WATER DISTRIBUTION NETWORKS**

2   G.P. Cimellaro[1], A.Tinebra[2], C.Renschler[3], M.Fragiadakis[4]

3   **ABSTRACT**

4   The increased frequency of natural disasters and man-made catastrophes has caused major disruptions to

5   critical infrastructures (CI) such as Water Distribution Networks (WDNs). Therefore, reducing the

6   vulnerability of the systems through physical and organizational restoration plans are the main concern

7   for system engineers and utility managers that are responsible for the design, operation, and protection

8   of WDNs. In this paper, a Resilience Index (R) of a WDN has been proposed which is the product of

9   three indices: (i) the number of users temporary without water, (ii) the water level in the tank, and (iii)

10   the water quality. The Resilience Index is expected to help planners and engineers to evaluate the

11   functionality of a WDN which includes: (1) delivering a certain demand of water with an acceptable

12   level of pressure and quality; (2) the restoration process following an extreme event. A small town in the

13   South of Italy has been selected as a case study to show the applicability of this index using different

14   disruptive scenarios and restoration plans. The numerical results show the importance of the partition of

15   the network in districts to reduce the extension of disservices. It is also shown the necessity to consider

16   the indices separately to find trends that cannot be captured by the global index. Advantages and

17   disadvantages of the different restoration plans are discussed. The proposed indices can be implemented

18   in a decision support tool used by governmental agencies which want to include the restoration process,

19   the environmental and social aspects in their design procedure.

20

21   KEYWORDS**:** Water Distribution Network, Disaster Resilience, Recovery, Resilience, Restoration,

22   Seismic Risk, Resilience index, Vulnerability, Infrastructure, Restoration Strategies

23   **INTRODUCTION**

[1] Visiting Professor, Department of Civil and Environmental Engineering, University of California Berkeley, Davis Hall, Berkeley, CA 94720-1710, USA (gianpaolo.cimellaro@polito.it)

[2] Graduate Research Assistant, Department of Structural and Geotechnical Engineering (DISEG), Politecnico di Torino, 10129 Turin, Italy (gianpaolo.cimellaro@polito.it)

[3] Associate Professor, Department of Geography, University at Buffalo (SUNY), 116 Wilkeson Quad, Buffalo, NY 14261, U.S.A. email: rensch@buffalo.edu

[4] Lecturer, School of Civil Engineering, National Technical University of Athens, email: mfrag@mail.ntua.gr

24 The water distribution networks and the Critical Infrastructures (CI) in general provide services by

25 allowing flows of fuels, materials, information, electric power etc.. The *disruptions* change the

26 operability state of parts of the network (e.g. nodes and/or links), and then the *recovery actions* restore

27 the functionality of the damaged parts of the network, allowing the performance of the system to return

28 to the nominal levels as fast as possible. In the past, emphasis was given to the physical protection of

29 water distribution networks, but now attention is shifting toward the infrastructure resilience, defined as

30 the ability of infrastructure systems to withstand, adapt to, and rapidly recover from the effects of a

31 disruptive event. This concept is becoming increasingly important in the context of CIs and defining

32 infrastructure functionality is essential for evaluating its resilience (Cimellaro et al., 2014a). Although

33 several authors (Holling, 1973; Mileti, 1999; Fiksel, 2003) have worked in the field of Disaster

34 Resilience, Bruneau et al. (2003) offered the first broad definition of this quantity including the effects

35 of losses, mitigation and rapid recovery. In their study, they identify four dimensions of community

36 resilience, namely: i) *technical*, ii) *organizational*, iii) *social*, and iv) *economic*. However, in their work

37 they did not provide a detailed quantification of it, but rather a collection of quantitative performance

38 criteria for each property. After the general framework provided by Bruneau et al., various studies have

39 been carried out, with the goal of evaluating resilience and identifying its main units of measurement.

40 For example, Cimellaro et al. (2005, 2010a), formulated the first framework to quantify resilience,

41 where uncertainties in the intensity measures were considered. Chang and Shinozuka (2004) refined the

42 method proposed by Bruneau (2003), by proposing a metric of system performance Q, which is

43 evaluated comparing the extreme events scenario with the normal operating conditions and they applied

44 the method to the case study of the Memphis water system. Miles and Chang (2006) presented a

45 comprehensive conceptual model of recovery, which establishes the relationships between a

46 community's household business, lifeline networks and neighborhoods. Even if a measure of resilience

is not provided in their work, the paper points out the necessity to correlate the concept of recovery to real factors, such as household income, the year the structure was built, etc.. The same year Cagnan et al. (2006) has developed a model of post-earthquake restoration processes for an electric power system. A discrete event simulation model based on available data has been built, with the goal of improving the restoration processes in future earthquakes.

Several authors have used the resiliency concept as input in *decision support methodologies* that assist authorities in prioritizing infrastructure investments for disaster mitigation, emergency response and recovery activities. In particular, it has been applied to *hospitals* (Cimellaro et al., 2010b; Cimellaro and Pique`, 2014a), *lifeline structures* (Ouyang and Duenas-Osorio, 2011, Cimellaro et al., 2014b; Ouyang, 2014) and *cities* (Chang et al, 2014) using different optimization methods based on *economic* (Chang and Shinozuka, 2004), *downtime* (Cagnan et al., 2006) or *multi-criteria analysis* (Javanbarg et al., 2008). Recently Cimellaro et al. (2014c) have developed a new methodology to evaluate resilience on physical infrastructures including their interdependencies using time series analysis and applying it to the 2011 Tohoku earthquake in Japan.

According to the literature, several methods are available for quantifying resilience of infrastructure systems which can be grouped in *probabilistic methods* (Miller-Hooks et al, 2012, Queiroz et al., 2013), *graph theory methods* (Berche et al, 2009; Leu et al., 2010, Dorbritz, 2011), *fuzzy methods* (Heaslip et al., 2010) and *analytical methods* (Cimellaro et al., 2010; Tamvakis and Xenidis, 2013).

Miller-Hooks et al. (2012) proposed a non-linear, stochastic program addressing an integer L-shaped method associated with Monte Carlo simulations to quantify resilience. However, the method is computationally unaffordable for real systems which include a large number of interdependent nodes. Dorbritz (2011) combined the approach of Bruneau et al. (2003), with network analysis and proposed a resilience quantification method that tries to introduce, also, the complex network concepts introduced

70   by Berche et al. (2009) for the public transportation network. Heaslip et al. (2010) developed a method

71   to assess and quantify resilience using Fuzzy Inference Systems (FIS). In particular, they developed a

72   hierarchically structured dependency diagram of variables that can represent the performance hierarchy

73   levels. However, the use of more intuitive values for variables that quantify resilience may have an

74   effect on the accuracy of assessments and may complicate the decision making process. Furthermore, a

75   complete FIS should include a large number of variables and rules which might make the method

76   computationally unaffordable. Recently, Tamvakis and Xenidis (2013) proposed a framework based on

77   entropy theory concepts. Entropy describes the system's disorder at a given point in time and it is

78   measurable in a single metric analogously to resilience which describes the system's potential to recover

79   to a desired system's condition. Although the idea seems promising, they fail to provide details about

80   the method and applications which show the feasibility of the methodology.

81   When considering the *reliability of infrastructures,* the different methodologies available in literature

82   can be grouped in two main categories: (i) *simulation-based models* and (ii) *analytical methods* (Kim et

83   al., 2010). (i) Simulation-based models involve the use of random sampling techniques and Monte Carlo

84   simulation to approximate system functionality. For example, Wang and O-Rourke (2008) characterized

85   the performance of a large water supply system in term of system reliability and serviceability. They

86   use probabilistic seismic hazard analysis, theoretical and empirical relations to estimate pipeline

87   response. (ii) Analytical methods do not require repeated sampling and therefore they allow more rapid

88   computations, but they are based on assumptions that sometimes might not fit to the problem at hand

89   (Francis and Bekera, 2014; Davis, 2014).

90   In the last decade, several metrics have been proposed in literature to measure the performance of

91   WDNs. A good state of the art is available in Jalal (2008). For example, Todini (2000) proposed an

92   index which is a measure of the capability of the network to cope with failures and it is related indirectly

93   to system reliability.   Other authors have also extended this resilience index to overcome certain

94   drawbacks (Prasad and Park, 2004; Jayaram and Srinivasan, 2008), such as the inapplicability of the

95   index in networks with multiple sources.   They have listed the theoretical advantages of their

96   approaches, but none of them has compared the performance of these resilience indices.   Recently,

97   Davis (2014) in his work has defined 5 categories of water services. He has compared pre and post-

98   disaster services and has distinguished between operability and functionality.   Of course, the literature

99   review presented above cannot be comprehensive, but many of the works cited are based on the review

100   of previous works to quantify resilience, therefore it is still adequate to identify the different trends to

101   quantify resilience of infrastructures.

102   In this study, a Resilience Index (R) for a water distribution system has been proposed to measure

103   its performance. The proposed index R is defined as the product of three indices: one describes the

104   demand and is based on the number of users temporary without water (R_1); the second describes the

105   capacity and is based on the tank water height (R_2); the third (R_3) is based on the water quality.   These

106   indices will help planners and engineers to evaluate the functionality of a water distribution system

107   which consists in delivering a certain demand of water with an acceptable level of pressure and quality.

108   A small town located in a seismic region in Italy, has been used as a case study. The WDN has been

109   analyzed using the software EPANET 2.0 (Rossman, 2000) and different restoration plans have been

110   compared using the proposed resilience indices.

RESILIENCE OF WATER DISTRIBUTION NETWORK

112   The definition that has been used in this paper to quantify resilience of the WDN is the one provided in

113   the work of Bruneau et al. (2003) where resilience is defined as the *ability of a system to reduce the*

114   *chances of shock, to absorb such a shock if it occurs and to recovery quickly after a shock*.   Later the

115   same definition has been quantified and extended by Cimellaro et al. (2010a, b), where the resilience

116   index (R) has been defined as *a function indicating the capability to sustain a level of functionality for a*

117   *given building, bridge, lifeline networks, or community, over a period defined as the Control Time (T_{LC})*

118   *that is usually decided by owners, or society (e.g. life cycle of the system, etc.).* An essential parameter

119   for the definition of Resilience of the WDN is the definition of functionality/performance index which is

120   provided in the next paragraph.

121   **Definition of a new performance index for Water Distribution Networks**

122   Earthquake effects on water supply systems have been investigated extensively in literature and different

123   methodologies for estimating the reliability and serviceability of water supply systems heavily damaged

124   by earthquake are available in literature (Ballantyne et al., 1990; Taylor, 1991; Shinozuka et al., 1992;

125   Markov et al., 1994; and Hwang et al., 1998). The proposed index is composed of three parts which

126   depend on the number of households that would suffer water outage, the tank water level and the water

127   quality. The first part of the index is proportional to the system serviceability index (SSI) proposed by

128   Todini (2000), which is defined as the ratio of the sum of satisfied water demands after an earthquake to

129   that before an earthquake. In detail, three performance functions $F_1(t)$, $F_2(t)$ and $F_3(t)$ have been

130   presented. $F_1(t)$ relates to the number of households without water, therefore it is related to the *social*

131   *dimension* of the resilience problem. Analytically it is defined as

132    $$F_1(t) = 1 - \frac{\sum_i n_{p,e}{}^i}{n_{Tot}} \quad \text{for} \ \ i = 1 \ldots n \tag{1}$$

133   where $n_{p,e}{}^i$ are the equivalent number of users for each node that suffer insufficient pressure, n_{Tot} are the

134   total number of users within the distribution system, n is the total number of nodes that suffer water

135   outage. The Loss Function $L_1(I, T_R)$ is defined as

136    $$L_1(I, T_R) = \frac{\sum_i n_{d,e}{}^i (I, T_R)}{n_{Tot}} \quad \text{for} \ \ i = 1 \ldots n \tag{2}$$

137   where $n_{d,e}{}^i$ are the number of *Demand Nodes* which are assumed directly proportional to the water

138   volume lost W_{Lost} during the extreme event and the repair operations; I is an intensity parameter; T_R is

139   the recovery period which is defined as the period necessary to restore the functionality of a system to a

140   desired level that can operate or function the same, close to, or better than the original one (Cimellaro et

141   al, 2010). In detail, $n_{d,e}{}^i$ is given by the following equation

142    $$n_{d,e}{}^i = n_i \cdot \frac{W_{Lost}{}^i}{W_i} \tag{3}$$

143   where i indicates the general node in which the pressure is insufficient to ensure the demand water flow;

144   n_i is the total number of entities connected to node i; $W_{Lost}{}^i$ is the water volume lost and W_i is the water

145   volume that the entities would consume in normal operating conditions. To evaluate the volume of water

146   lost and the volume of water in normal operating conditions, the following equations have been used

147    $$W_i = \int_{t_j}^{t_{j+1}} Q_{Demand}(t)dt \tag{4}$$

148    $$W_{Lost}{}^i = \int_{t_j}^{t_{j+1}} [Q_{Demand}(t) - Q_i(t)]dt \tag{5}$$

149   where t_j and t_{j+1} are generic instants after the extreme event ($t > t_1$); Q_{Demand} is the water demand flow at

150   the instant t and Q_i is the real water flow at the time t afterwards the damage of the pipe. For a given

151   extreme event, the general form of $F_1(t)$ is shown in Figure 1a. The control time T_{LC} has been divided in

152   four different period ranges. T_{NF-I} is the normal operating functionality period before the earthquake; T_M

153   is the operating period range immediately after the earthquake and before the first emergency

154   operations; T_E is the transition period when the water system is partially in service; T_{NF-II} is the normal

155   operating functionality after the repair operations. Moreover, t_1 is the time instant when the extreme

156   event occurs, t_2 is the time instant when the damaged pipe is isolated, t_3 is the time instant when the

157   repair operations are finished and t_4 is a generic instant when the system works in normal operating

158 conditions. The difference between t_3 and t_1 corresponds to the Recovery Time T_R. Then the restoration

159 process has been divided in two phases: *Phase I* is the time interval necessary for the first emergency

160 operations and the isolation of the area where the damage happens, while *Phase II* is the time interval

161 necessary for the repair operations. During *Phase II*, the users are temporary without water, so, in this

162 case, the water flow is equal to zero, while the ratio $W_{Lost}{}^i / W_i$ is equal to 1, since $n_e{}^i = n_i$. Therefore,

163 after the definition of the performance index $F_1(t)$ given in Equation (1) the corresponding resilience

164 index is defined as

165
$$R_1 = \int_0^{T_{LC}} \frac{F_1(t)}{T_{LC}} dt \tag{6}$$

166 where $F_1(t)$ is the performance function proportional to the number of equivalent households n_e w/o

167 service; T_{LC} is the control time.

168 The second performance function $F_2(t)$ relates to the tank water level, which is directly related to the

169 reserve capacity of the tank and therefore to the *technical dimension* of the resilience problem. The

170 analytical expression is defined as

171
$$F_2(t) = \begin{cases} \dfrac{h(t)}{h_{Reserve}} & h \le h_{Reserve} \\ 1 & h > h_{Reserve} \end{cases} \tag{7}$$

172 where $h(t)$ is the water level in the tank at a given instant of time, while $h_{Reserve}$ corresponds to the

173 reserve capacity in the tank. In detail, if the water level is above the height corresponding to the reserve

174 capacity $h_{Reserve}$, $F_2(t)$ is equal to 1, but if the level decreases below $h_{Reserve}$, $F_2(t)$ has a value less than 1.

175 In this case, the Loss Function $L_2(I, T_R)$ is given by

176
$$L_2(I, T_R) = 1 - \frac{h(t, I, T_R)}{h_{Reserve}} \tag{8}$$

177   The loss function given in Equation (8) provides information about how much water has been lost

178   during the earthquake and allows establishing what is the optimal strategy to recover the Reserve

179   Capacity.

180   The definition of performance function in equation (7) can be generalized and extended not only to

181   tanks, but also to pumps, by using the "Hydraulic head" or "Piezometric head" which is a specific

182   measure of liquid pressure that can also be used for pumps.

183   With respect to Equation (2), for Equation (8) is not possible to define a fixed recovery time before the

184   numerical simulations, because in this case T_R is directly related to the type of restoration plan adopted.

185   In Figure 1b is shown a sketch of how $F_2(t)$ looks like. The figure shows how $F_2(t)$ doesn't return to 1 at

186   the end of T_{LC} , but it can assume lower values, if a proper restoration strategy is not adopted. In this

187   case, the Resilience Index is given by

188
$$R_2 = \int_0^{T_{LC}} \frac{F_2(t)}{T_{LC}}\, dt \qquad (9)$$

189   where $F_2(t)$ is the water level in the tank; T_{LC} is the control time. Special attention requires the

190   definition of R_2 when multiple tanks are in the network. In this case, the index is given by

191
$$R_2 = \frac{\sum_i w_i R_2^{\ i}}{\sum_i w_i}; \quad i = 1,2 \qquad (10)$$

192   where w_i are the weight coefficients of the n tanks in the network. These coefficients can be evaluated

193   using two approaches. Assuming two tanks, in the first case, the weights w_1 and w_2 are proportional to

194   the average flow loss on the two pipes in which the connecting pipe is divided after the earthquake. In

195   the second case, the weights w_1 and w_2 are proportional to the reserve capacity.

196   Since WDNs have strict requirements of ensuring water quality, the global resilience index should also

197   include a water quality index which is related to the *environmental dimension* of the resilience problem.

198 Currently there is no globally accepted composite index of water quality. Most water quality indices rely

199 on normalizing, or standardizing data according to expected concentrations and some interpretation of

200 'good' versus 'bad' concentrations. Parameters are often then weighted according to their perceived

201 importance to overall water quality and the index is calculated as the weighted average of all the

202 observations of interest. The authors do not want to enter in the discussion of which index is better to

203 adopt, however once an index of water quality check Q is selected, it can be compared with its value

204 before the earthquake event defining the following performance function

205 $$F_3(t) = \frac{Q(t)}{Q*}$$ (11)

206 where $Q*$ and $Q(t)$ are the water quality indices before and after the seismic event respectively. The

207 final resilience index for water quality is defined as

208 $$R_3 = \int_0^{T_{LC}} \frac{F_3(t)}{T_{LC}} dt$$ (12)

209 Then the three indices are combined together to have a comprehensive evaluation of the WDN, so the

210 Global Resilience Index is defined as

211 $$R = R_1 \cdot R_2 \cdot R_3$$ (13)

212 The R index summarizes the performance of the WDN considering the demand R_1 (users), the capacity

213 R_2 (water level in the tank) and the water quality R_3.

214 The metrics has been multiplied, because the global index R in equation (13) is more sensitive to the

215 different scenario events when the three indices are multiplied. In fact some scenarios in the case study

216 below generate high values of R_1, so it seems that damage did not cause any effect, but in reality the

217 quantity of water loss has been relevant and this cause a reduction of the water reserve capacity in the

218 tank and consequently of R_2.

CASE STUDY

220 The methodology described above has been applied to the WDN of Calascibetta, an italian town

221 supplying 4600 inhabitants in the Enna Province, located on Erei Mountains (Figure 2) in Sicily.

222

223 **Seismic hazard in the region**

224 The town did not suffer high intensity earthquakes except the '*Noto valley earthquake*' which occurred

225 in 1693 and produced severe damages in the entire eastern side of the island. Its intensity was about *XI°*

226 *of Mercalli–Cancani–Sieberg (MCS)* scale, but in Calascibetta the intensity felt was about *VII°*. Using

227 the Neo-deterministic seismic hazard scenario proposed by Panza et al. (2012), the value of the peak

228 ground velocity in the town of Calascibetta (14.4000 N 37.4000 E) is in the range between 15 and 30

229 cm/sec (Panza et al., 2014a). The Neo-determinist approach has been preferred with respect to the

230 Probabilistic Seismic Hazard analysis (Cimellaro et al., 2011), because the former provides non

231 conservative results (Panza et al., 2014b) at the specific site. The PGV used in the analysis is the

232 average value of 22.5 *cm/s*, which can be assumed constant over the entire WDN, because of the limited

233 extension of the network.

234

235 **Characteristics of the water distribution network**

236 The WDN consists of two tanks:

237   1. the *roof tank* (Capacity = 50 m^3) located in the highest part of the town;

238   2. *St. Peter's tank* (Capacity = 500 m^3), which is supplied by the pipes coming from the roof tank.

239 The water source capacity of the two tanks is the reservoir located at Ancipa Dam. The water is pumped

240 at the roof tank from a station located at the bottom of the hill and from there, the water is distributed to

241 district 1 and to St. Peter tank which supplies the entire city. The paper deals only with the distribution

242 network, while the adduction network in not considered in the analysis. The entire network is made by

243 polyethylene pipes which are characterized by an easy process of installation, high elasticity that allows

244 it to absorb modest land subsidence without damage on the structure, chemical inertness against the

245 aggressiveness of land or percolated water or liquids conveyed. In

246 Figure **3** is shown the plan view of the WDN of Calascibetta which is divided in eight districts. All

247 districts are connected through pipes which are normally closed in normal operating conditions, but they

248 can be open in case of an emergency. Three diameters of respectively 63, 110, 160 *mm* are installed in

249 the network, while 32 *mm* diameter pipes have been used to connect the different services within the

250 building.

251 The length of the 32, 63, 110 and 160 mm diameter pipes are respectively 3728.83m, 8719.35m,

252 4427.65 and 1115.35m. Pressure reducing valves (*PRV*) have been installed in the network to maintain

253 the pressure within certain limits which are given in Table 1, while shut-off valves have been installed to

254 close the pipes in case of an emergency (

255 Figure **3**).

256

257 **Model description, assumptions and calibration**

258 The WDN of Calascibetta has been modeled using EPANET 2.0 (Rossman, 2000). The standard

259 procedure used in the software to evaluate the nodes' pressure and the flow in each pipe is the Demand

260 Driven Analysis (*DDA)*. However, the limitation of this method is that the demand flow is fixed a priori

261 in each node, so the DDA provides the same value of demand flow even if the pressure is below the

262 threshold necessary to satisfy the demand in the WDN. For these reasons, the DDA works well in

263 normal operating conditions when there are no failures in the pipes, but if one pipe fails, the pressure in

264 some nodes could be below the threshold value necessary to satisfy the demand. In this case, the

265 Pressure Driven Analysis (PDA) has been used. So all the simulations with pipe failures start with a

266 *DDA* analysis and when the pressure in one node goes below the threshold necessary to satisfy the

267 demand flow, it is transformed in a *Emitter* node (Rossman, 2000). The PDA analysis in presence of

268 Emitters is characterized by less flow circulating in the network and consequently by reduced hydraulic

269 head losses when compared with the first analysis (DDA). In the analysis, the pressure necessary to

270 satisfy the demand flow at each node is set to 20 *m* of water column (2 *bar)*,so that at least 5 *m* of water

271 column are above the tallest house in Calascibetta which has an height of about 13 m. The *Darcy-*

272 *Weisbach* formula has been used to evaluate the head losses which are given by

273 $$h = \lambda(\varepsilon, d, q) \frac{L \cdot v^2}{d \cdot 2g} \qquad (14)$$

274 where λ is the friction factor (depending on the roughness ε, the diameter d and the flow rate q), L is the

275 pipe length, v is the flow velocity, g is the acceleration of gravity. The friction factor λ is estimated with

276 the use of different equations as a function of the *Reynolds Number* (*RE*). The roughness ε for the

277 polyethylene pipes has been assumed constant and equal to 0.005 *mm*, because the pipes have been

278 recently installed and in general, the polyethylene material maintains its hydraulics characteristics. The

279 concentrated losses have been neglected. Pipes with the same features (e.g. diameter, roughness) have

280 been combined into a single pipe with length equal to the sum of the lengths of each pipe. The pipes

281 with diameter of 32 *mm* connecting to the services have been neglected. The roof tank has a cylindrical

282 shape with a diameter of 3 m, while St.Peter tank is composed by two tanks of rectangular shape that

283 cover an area of 66 *m²* each. To simplify the modeling in EPANET the rectangular tank has been

284 replaced with an equivalent tank with a diameter of 12.95m that have a cylindrical shape of the same

285 volume ($D = \sqrt{4A/\pi} = \sqrt{4 \cdot 132/\pi} \cong 12.95m$). The variation of water flow demand over the 24 hours has

286 been determined using the data provided from the operator from *July 2011* to *June 2012*. In particular,

287 the water flow demand is obtained as average of a monthly time pattern for each district. For example,

288 Figure 4 shows the water flow demand related to District 1. Pipe breaks and leaks have been modeled

289   in EPANET using the scheme shown in Figure 5, however simulations have been focusing only on pipes

290   breaks which are assumed to happen in the middle point of the pipe. Then at the end-parts of the

291   divided pipe, two reservoirs are added to simulate the water flow through the crack. The tanks have a

292   hydraulic head equal to the elevation of the break point which is evaluated with a linear interpolation

293   between the two nodes of the original pipe. Finally, a valve is inserted on each new pipe so that the

294   water can only flow from the broken pipe to the tanks and not vice versa.

295

Seismic Damage Model for water pipes

297   Pipeline damage models for the seismic vulnerability assessment are usually formulated as the repair

298   rate for unit length of pipes. These models can be derived from the data collected during previous

299   seismic events or any other hazard which produced breakages in the pipes. In this research, the well

300   known model in the American Lifeline Alliance (ALA, 2001) has been used. In particular, the repair rate

301   is defined as

302   $RR = K(0.00187)PGV$ (15)

303   where RR is the Repair Rate which is the number of pipe breaks per 1000 ft (305 m) of pipe, K is a

304   coefficient determined by the pipe material, pipe joint type, pipe diameter, type of fitting and soil

305   condition and the PGV is the peak ground velocity which has the units in in/s. K is assumed 0.5,

306   because in Calascibetta are polyethylene pipes and the type of fitting adopted is rubber gasket, while the

307   PGV is assumed equal to 22.5 cm/s (8.86 in/s). So applying Equation (15), the value of RR is equal to

308   0.008. Furthermore, the WDN of Calascibetta consists of pipes of different importance, which have

309   been distinguished in four groups: (1) *main pipes*, (2) *pipes at the entrance of each district*, (3)

310   *connecting pipes* and (4) *plain pipes within each district*. In order to take into account the different

311   importance of each pipe Equation (15) has been modified introducing the importance factor (I_m), thus

312   $RR = I_{\mathrm{m}}K(0.00187)PGV$ (16)

313   where I_{m} is assumed equal to *2, 1.5, 1* and *0.8*, respectively. Finally, the probability of having a number

314   *n* of breakages in a pipe of length *L* is given by the following expression

315   $P(n) = \dfrac{(RR \cdot L)^{n}}{n!} e^{-RR \cdot L}$ (17)

316   where *n* is the number of pipe breaks, *RR* the repair ratio evaluated using Equation (16) and *L* is the

317   length of pipe (expressed in terms of 1000-ft segment USCS). Figure 6 shows the probability of having

318   a certain number of breaks in the WDN of Calascibetta. The figure justifies the choice of selecting the

319   scenarios with a single break, because the probability of having two breaks is negligible.

320

321   **Risk of pipe failure**

322   The risk of failure of a WDN can be obtained using its topology and the failure probability $P(n)$ of every

323   pipe. The failure to deliver a sufficient amount of water from an inflow node *i* to an outflow node *j*, can

324   be defined as the probability that the hydraulic head goes below a specified threshold value. Therefore,

325   the probability of failure of a network can be obtained after the hydraulic analysis of a damaged

326   network. Then Monte Carlo simulations are employed reducing the network topology by removing the

327   pipes segments based on the failure probability of every pipe $P(n)$. Once the failed pipes are removed,

328   an algorithm based on Graph Theory can be used to determine whether a path between an inflow and an

329   outflow node exists. For every damaged network created, Monte Carlo simulations have been employed

330   using 5000 runs in order to calculate the statistics of the hydraulic quantities of interest. The procedure

331   is discussed in detail in Fragiadakis and Christodoulou (2014).

332

333   **Selection of scenarios event**

334 Classical risk analysis has different assumptions, objectives and methods which are not sufficient for

335 resilient design, so the departure from the traditional design practices are needed (Park et al., 2013).

336 Resilience is a dynamic quantity that must be constantly managed and is characterized by a lack of

337 certainty. The uncertainty of potential future disruptions makes the use of scenarios important. In this

338 work, four types of scenarios that cover a wide range of potential occurrences for the WDN of

339 Calascibetta have been selected based on a "*hybrid approach*" which combines Monte Carlo based

340 algorithm with engineering judgment. The Monte Carlo based algorithm allows assessing the

341 preliminary failure probabilities in various locations within the network. The reason for combining the

342 engineering judgment in the approach lies on the topology of the WDN of Calascibetta. The network is

343 divided in 8 districts connected with a main pipe and several connecting pipes.

344 The main pipe and the connecting ones are important because if they fail, the entire district will remain

345 without water, so additional scenarios have been selected for explicitly assessing their significance.

346 However, the failures within the district of smaller diameter pipes have been also selected.

347 Four groups of scenarios (S_1, S_2, S_3 and S_4) have been selected to examine the effect of different types of

348 pipe failures. S denotes a "Scenario" and the subscript number indicates the group to which each

349 scenario belongs (

350 Figure **7**). In detail, the following groups of scenarios in Table 2 have been analyzed:

351   1. Group S_1 includes scenarios with one break on the main pipeline and the supply pipe of the St.

352   Peter Tank;

353   2. Group S_2 includes all scenarios with breaks in the supply pipes of each district;

354   3. Group S_3 includes all scenarios where the breaks occur in the districts;

355   4. Group S_4 includes all scenarios where the breaks occur in the connecting pipes.

356 Within group S_3, the scenarios inside each district have been selected, so that the impact of pressure drop

357 and of the number of users affected is maximized. Typically, eight damaged events for every district

358 have been randomly created, with the exceptions of *District 7* where six scenarios have been selected

359 and *District 1* where 12 scenarios have been selected (the largest district). Figure 8 shows the scenarios

360 considered for *District 6*, while in Figure 9 are plotted the average pressures for each scenario and

361 compared to the average pressure in normal operating conditions. During the selection of the scenarios

362 for every District, generally it is noticed that the peripheral areas inside each District have less influence

363 on the global district pressure when one pipe fails. However, other factors can also affect the scenario

364 selection such as the *topographic features* of the district, the *number of users* and the *valve distribution*

365 etc. For example in District 1, because for almost all the assumed scenarios the average pressure level is

366 the same, the scenario with the highest number of users without water service has been selected.

367

368 **Recovery time and restoration process**

369 In the case study, the control time T_{LC} is assumed equal to 48 hours which is the time to repair the

370 damaged pipe according to the emergency plan of the Water distribution Provider in the region.

371 According to the information provided by the operator (AcquaEnna S.C.p.A) of the WDN, after the

372 earthquake, the first emergency operations (e.g. isolate the zone where the pipe is damaged) are realized

373 within 1 hour, while the repair operations, if the diameter is less than 600 *mm*, are realized in maximum

374 12 hours. Additionally other 24 hours has been added, because that is the time necessary to inform in

375 advance the residents of the repair operations. Finally, T_R has been assumed equal to 38 hours (one

376 hour has been added to include the uncertainties) and it is assumed constant for all the simulations.

377

378 **Numerical results and lesson learned**

17

379   In Table 3 are summarized the resilience indices according to Equation (6), (9) and (13) for the different

380   scenarios selected. In the analyses, it is assumed that the water quality check (e.g. hardness, presence of

381   contaminants, etc.) remains above the standards defined by the law and constant before and after the

382   repair, therefore the index R_3 is not shown in the results. The index R_1 is function of the number of

383   households without water and it is lower in the districts where the pipe failure is selected, while it

384   remains constant in other districts, because the effect of the pipe failure is confined in the district using

385   valves. As expected, the lowest value of R_1 index is obtained with scenario 1, which corresponds to

386   failure in the main pipeline. In this case, the seven districts supplied by the main pipeline, remain

387   without water until the pipeline is repaired. This generates a drop of the function $F_1(t)$ and therefore of

388   R_1. The same observation applies to scenarios 21 and 28 that involve the main pipeline. The index R_2

389   instead is more sensitive than R_1 for the selected scenarios, because is affected by the volume of water

390   loss which is function of the *pipe diameter* and the *location of the breakage*. In fact, if the breakage

391   affects a pipe which provide water to several households, during the repair operation when the pipe is

392   isolated, the water tank level increase and so the value of R_2. For example, during Scenario 1, which

393   corresponds to the main pipeline failure, the entire pipe is isolated and all districts are without water.

394   Consequently, the water level in the tank increases because the seven districts are without water supply,

395   and then the R_2 index increases. Scenario 9 (breakage at the input pipe of district 8) is the worst in term

396   of R_2, because for the particular position of this pipe and for its diameter (110 *mm*), the flow rate loss is

397   about 75 *l/s* and this leads emptying St.Peter Tank. Because both indices are equally important to

398   describe certain scenarios, they have been combined together in a global index R which is the synthesis

399   of the information obtained from R_1 and R_2. Further considerations are necessary for the scenario 18

400   when the Index R_2 is evaluated. In this case, the failure is in the pipe connecting District 1 which is

401   supplied by the Roof Tank and District 2 which is supplied by St.Peter Tank, therefore, the index R_2 is

402   determined using a weight average which is given in Equation (10) where w_1 and w_2 are weight

403   coefficients of the Roof Tank and St.Peter Tank respectively.

404   Following the two approaches mentioned in previous section, the weights w_1 =0.3274 and w_2 =0.6726

405   are determined using the first approach, while w_1 =0.0693 and w_2 =0.9307 are determined using the

406   second approach when they are proportional to the reserve capacity which is 31.62 m^3 for the Roof tank

407   and 424.82 m^3 for San Peter tank, respectively. However, in all tables and figures the results related to

408   scenario 18 refer to the second approach, which is more general. The sensitivity of the Resilience

409   indicators (R_1, R_2 & R) to the time of the earthquake occurrence during the day is shown in

410   Figure **10** for the scenario 9. The Resilience Index R_2, instead, doesn't have any significant variations

411   with respect to the earthquake occurrence during the day. Instead, for index R_1, if the earthquake occurs

412   at 1 am and failure corresponds to scenario 9, then St.Peter tank is empty, because of the flow rate loss.

413   However, because in the evening the demand flow is less than the input flow, the tank starts increasing

414   its water level and in 24 hours is able to cover the total demand flow. Instead, if the earthquake occurs

415   at 6 am, the demand flow has its peak and the tank in less than 2 hours decreases its water level until it

416   empties to cover the demand and the flow rate loss. From that moment, the tank remains empty,

417   because the demand flow continues to be higher than the input flow. Only when the output flow is less

418   than the input flow, then the water level starts increasing (

419   Figure **10**).

420

421   **Restoration plans**

422   Three different restoration plans have been proposed. The *first restoration plan* involves the closure of

423   the tanks until the entire reserve capacity is recovered. The minimum and the maximum variation of

424   recovery time T_R to restore the full capacity in the tanks for the different scenarios are plotted in Figure

425   11. Please note that for the scenarios 1, 2, 10, 21, 28 and 29 the recovery time is not shown, because the

426   reserve is automatically recovered during the time interval T_{LC}.

427   The maximum and the minimum recovery time in Figure 11 has been evaluated using the procedure

428   described in Figure 12 for scenario 12 where is plotted the tank water height vs. time (hours) right after

429   the earthquake. The bold line represents the water level in normal operating conditions, while the gray

430   line the water level when no recovery strategies have been applied. At the end of the control time T_{LC},

431   the final water height h_{Final} will be less than the reserve height $h_{Reserve}$ (4.47 *m* for the Roof Tank, 3.23 *m*

432   for St. Peter Tank). This is happening because in normal operating conditions, the final water height is

433   higher than the water reserve height, because the reserve capacity of the tank is not used. However,

434   when the pipe fails the water reserve capacity of the tank is used to satisfy the water demand, so the final

435   water height will be lower than the water reserve height. The difference between these two values ($\Delta h=$

436    $h_{Reserve}$ - h_{Final}) has led to the construction of the gray dashed line in Figure 12 that is the target to reach

437   for recovering the reserve capacity. In particular, the grey line (No restore) is translated of Δh to have a

438   curve that follows the water demand and that reaches the $h_{Reserve}$ at the end of the 48 hours. The others

439   curves correspond to different instants when the tank is closed. The straight lines derive from the

440   assumption of constant water flow in the tank when it is closed, therefore they can estimate the time

441   interval to recover the reserve capacity and when the entities suffer water outage. For example, for

442   scenario 12, the maximum recovery time is 13 hours and the minimum is 6 hours. The minimum and the

443   maximum recovery time will depend on Δh. With the restoration strategy above, no other costs of

444   electricity due to the use of pumps must be added, but in that time interval, the users remain without

445   water supply.

446   The *second restoration plan* involves the use of the maximum available flow from the pump

447   station. In normal operating conditions, the input flow to the distribution system is about 5.44 *l/s*.

448   Neglecting the physiological water losses, the input flow in the roof tank is around 1.16 l/s, while the

449   input flow in the St.Peter tank is 4.28 l/s. In emergency conditions, the pump station can supply a

450   maximum flow of 19 l/s. With this flow rate, the recovery times of the reserve capacity have been

451   calculated for the selected scenarios, using the following equation

452
$$\frac{\Delta h \cdot A_T}{\Delta t \cdot (Q_e / 1000)} = T_R(h) \tag{18}$$

453   where $\Delta h = h_{Reserve} - h_{Final}$ in m, A_T is the tank's area in m^2, Q_e in l/s is the available flow to be added to

454   recover the water reserve capacity, Δt is equal to 3600 s. In Figure 13 are shown the values of the

455   recovery time T_R for the second restoration plan. In the selected scenarios, the total reserve capacity

456   which is recovered corresponds to the one of St.Peter Tank, that is equal to Q_e = 13.56 l/s, where Q_e=

457   (19-1.16-4.28) = 13.56 l/s. Please note that for the scenarios 1, 2, 10, 18 and 28 the recovery time is not

458   shown, because the reserve is automatically recovered. The higher recovery times are obtained for the

459   scenarios with the lowest h_{Final} and consequently the lowest R_2 values. With this strategy, the recovery

460   time T_R is reduced, but the cost of electricity, deriving from the use of pumps is increased.

461   The *third restoration plan* is a hybrid combination of the first two strategies. First, the water tank

462   is closed for the first seven hours in the morning and then part of the available flow is used for

463   recovering the water reserve capacity. The advantage of this restoration plan is based on the limited use

464   of the available flow from the pump station and the reduced amount of downtime for the water tank,

465   which is going to be closed only in the early morning, generating less discomfort for the residents. The

466   available flow Q_e is obtained using the following equation:

467
$$Q_e = \frac{\Delta h \cdot A_T}{\Delta t \cdot T_R} \tag{19}$$

468   where the recovery time T_R is equal to 7 hours (fixed), while $\Delta h = h_{Reserve} - h_{Final}$ will be higher than the

469   value obtained in the second strategy, because the final water height increases after the closure of the

470 tank. This strategy can be adopted for those scenarios where the recovery time T_R is higher with respect

471 to the other two strategies. Please note that in the third strategy the recovery time T_R is measured as sum

472 of the period the tank is closed plus the period the pumps are operating. The use of the third restoration

473 strategy produces an increase of the R_2 value, but also produces a decrease on R_1 value caused by the

474 closure of the tank. The combined index R given in Equation (10) does not change with respect to the

475 condition when no retrofit strategies are applied. For example, in *scenario 12* the R_2 for the Minimum

476 Recovery Time (6 hours) is 0.82; the corresponding R_1 is equal to 0.87 and then the combined index R is

477 0.71, which is the same when no restoration plans are taken into account.   In this case, it is

478 recommended to work with only one of the two indices to appreciate the effect of the retrofit strategy

479 proposed. These considerations bring also to the conclusion that the third restoration plan should be

480 used only for scenarios where the recovery time T_R is short (e.g. scenarios 13, 15 and 29). The use of

481 the second or third restoration plan produces an overall improvement of the indices as shown in Figure

482 13 and Figure 14. In fact, with these strategies the index R_2 improves, while the index R_1 is maintained

483 at the same level in the second strategy, and it undergoes a slight reduction in the third strategy. The

484 improvement of the global index R with respect to the initial condition shows the validity of the selected

485 retrofit strategies (Figure 15).

486 Between the scenarios selected, *scenario 18* is interesting, because in this case the two tanks (Roof and

487 St.Peter) are working in parallel at the same time. This implies that the three restoration strategies should

488 be applied on the two tanks simultaneously. For the first strategy, the recovery time T_r for the roof tank

489 is between 3 and 9 hours, while for St. Peter tank is between 9 and 15 hours. For the second strategy,

490 using the same weight coefficients described above, the flow in the roof tank and the flow in St.Peter

491 tank are determined as weight average of the maximum available flow $Q_e = 13.56$ *l/s*. Using the second

492 restoration plan the recovery times are 5 hours and 16 minutes in the roof tank and 3 hours and 40

493   minutes in St. Peter tank. For the third restoration plan, the flow rate necessary to recover the reserve

494   capacity is Q_e is 0.31 *l/s* (h_{Final} = 3.52 *m*) for the Roof tank, while for St.Peter tank Q_e is 5.8 *l/s* (h_{Final} =

495   2.14 *m*).

496   *Scenario 29* requires also attention, because in this case the pipeline that supplies the St. Peter tank fails,

497   so the tank is able to provide water to the distribution system for the first 32 hours, but then it empties

498   before the repair operations finish. In this case, the most suitable restoration strategies are the second

499   and the third one. When the pipeline has been fixed, the incoming maximum available flow permits the

500   restoration of the reserve capacity in the water tank in about 9 hours. For the third restoration plan, the

501   available flow should be equal to 16.78 *l/s*. The restoration plan 1 can not be used, because when the

502   incoming pipe is under repair, no input flow can supply the tank which is closed, and the restoration of

503   the reserve capacity doesn't occur.

504   So the lesson learned is that applying one strategy with respect to the other depends on several

505   considerations such as the cost of electricity, the possibility to use the maximum available flow from the

506   pumps, the extension of the tank downtime and its effects on consumers, etc.. Although all these aspects

507   are very important, they have not been quantified in the selection of the optimal restoration plans and are

508   not been discussed in this paper, but they will be addressed by the authors in future research.

509   **CONCLUDING REMARKS**

510   A new resilience index R to measure the performance of a water distribution network (*WDN*) is

511   proposed, which combines both the technical, the environmental and the social dimension of resilience.

512   The metric is based on the combination of three indices which are defined in term of functionality *F(t)*

513   and recovery time T_R. The proposed indicator not only considers the initial losses, but it also attempts to

514   assess the restoration process of the system. The sensitivity analysis of the global resilience index R to

different disruptions scenarios in the WDN of a small town in the south of Italy is presented. The numerical results in EPANET have shown the positive effect of the separation in districts of the network and the need to use the indices separately, because in some scenarios have been observed opposite trends. Three different recovery plans have been compared considering the different disruption scenarios using the proposed indices. Between the different restoration plans, the first one corresponding to closing the tank for the entire town should be used with caution, because if the recovery time is long, it can create widespread disservices to the residents. Therefore, it is suggested to use this plan only when the quantity of water loss due to the damage pipes is modest, and consequently the tank can recover its water level in few hours. Instead, the hybrid approach (third strategy) can be adopted for those scenarios where the recovery time T_R is higher with respect to the other two strategies. In fact, it produces both an increment of the R_2 index and a decrease of the R_1 index caused by the closure of the tank. The considerations introduced in this paper need to be further developed and expanded by the researchers and designers who deal with WDNs. In particular the proposed indicator could be easily included into a knowledge based Decision Support System aimed at helping the Governmental agencies in selecting the most appropriate design for WDNs, by incorporating also the environmental and social dimension in the design process.

REFERENCES

536

537 Ambraseys N. N., Douglas, J., Sarma, S. K., and Smit, P. M. (2005). "Equations for the Estimation of

538   Strong Ground Motions from Shallow Crustal Earthquakes Using Data from Europe and the

539   Middle East: Horizontal Peak Ground Acceleration and Spectral Acceleration." *Bulletin of*

540   *Earthquake Engineering*, 3, 1-53.

541 American Lifelines Alliance. (April 2001). "Seismic Fragility Formulations for Water Systems PART1-

542   Guidelines." *American Society of Civil Engineers (ASCE).*

543 Ballantyne, D. B., Berg, E., Kennedy, J. Reneau, R., and Wu, D. (1990). "Earthquake Loss Estimation

544   Modeling of the Seattle Water System." *Technical Report*. Kennedy/Jenks/Chilton, Federal Way,

545   WA, 139p.

546 Berche, B., von Ferber, C., Holovatch, T., and Holovatch, Y. (2009). "Resilience of public transport

547   networks against attacks." *European Physical Journal B*, 71(1), 125-137.

548 Bruneau M., Chang S., Eguchi R., Lee G., O'Rourke T., Reinhorn A. M., Shinozuka M., Tierney K.,

549   Wallace W., and Winterfelt D. v. *(2003). "*A framework to Quantitatively Assess and Enhance the

550   Seismic Resilience of Communities." *Earthquake Spectra, 19(4), 733-752.*

551 Cagnan, Z., Davidson, R. A., and Guikema, S. D. (2006). "Post-Earthquake Restoration Planning for

552   Los Angeles Electric Power." *Earthquake Spectra*, 22(3), 589-608.

553 Chang SE, Shinozuka M. *"Measuring improvements in the disaster resilience of communities".*

554   *Earthquake Spectra 2004;20(3):739–55*

555 Chang, S., McDaniels, T., Fox, J., Dhariwal, R., and Longstaff, H. (2014). "Toward Disaster-Resilient

556   Cities: Characterizing Resilience of Infrastructure Systems with Expert Judgments." *Risk Analysis*,

557   34(3), 416-434.

Cimellaro GP, Reinhorn AM, Bruneau M. *"Resilience of a health care facility" Proceedings of annual meeting of the Asian Pacific network of centers for earthquake engineering research. ANCER. 2005.*

Cimellaro G. P., Reinhorn A. M., Bruneau M. (2010 a). "Framework for analytical quantification of disaster resilience." *Engineering Structures*, *32: 11, 3639–3649.*

Cimellaro G. P., Reinhorn A. M., Bruneau M. (2010 b). "Seismic resilience of a hospital system." *Structure and Infrastructure Engineering*, *6: 1-2, 127-144.*

Cimellaro, G. P., Reinhorn, A. M., D'Ambrisi, A., and De_Stefano, M. (2011). "Fragility Analysis and Seismic Record Selection." *Journal of Structural Engineering, ASCE*, 137(3), 379-390.

Cimellaro, G. P., and Pique`, M. (2014a). "Seismic Performance of Health care facilities using Discrete Event Simulation Models." Computational Methods, Seismic Protection, Hybrid Testing and Resilience in Earthquake Engineering - A tribute to the research contribution of Prof. Andrei Reinhorn, Editors: Cimellaro G.P. & Nagarajaiah S. & Kunnath S., ed., Springer International Publishing AG, ed., Springer, Netherland, 3311 GX Dordrecht, 250 ISBN: 978-3-319-06393-5.

Cimellaro, G. P., Villa, O., and Bruneau, M. (2014b). "Resilience-Based Design of Natural gas distribution networks." *Journal of Infrastructure Systems, ASCE*, 10.1061/(ASCE)IS.1943-555X.0000204.

Cimellaro, G. P., and Solari, D. (2014c). "Considerations about the optimal period range to evaluate the weight coefficient of coupled resilience index." *Engineering Structures*, 69(2014), 12-24.

Davis, C. A. (2014). "Water System Service Categories, Post-Earthquake Interaction, and Restoration Strategies." *Earthquake Spectra*, 30(4), 1487-1509.

Dorbritz, R. (2011). "Assessing the resilience of transportation systems in case of large-scale disastrous events." The 8th International Conference on Environmental Engineering, Vilnius, Lithuania, 19-20 May 2011, 1070-1076.

582 Fiksel, J. (2003) Designing resilient, sustainable systems. *Environmental Science and Technology*

583   37(23): 5330-39.

584 Fragiadakis M., Christodoulou S.E. (2014) "Seismic Reliability Assessment of Urban Water Network"

585   *Earthquake Engineering and Structural Dynamics,* 43(3), 357-374.

586 GIRAFFE. (2008). "GIRAFFE USER'S MANUAL version 4.2 January 2008." Cornell University,

587   School of Civil & Environmental Engineering, Ithaca, NY.

588 Hwang, H. H. M., Lin, H., and Shinozuka, M. (1998). "Seismic Performance Assessment of Water

589   Distribution Systems." *Journal of Infrastructure Systems*, ASCE, Vol. 4, No. 3, 118- 125.

590 Heaslip, K., Louisell, W. C., Collura, J., and Serulle, N. U. (2010). "A sketch level method for assessing

591   transportation network resiliency to natural disasters and man-made events." The 89th Annual

592   Meeting of the Transportation Research Board, Washington, D.C., U.S.A., 10-14 January 2010.

593 Holling, C. S. (1973) Resilience and Stability of Ecological Systems. *Annual Review of Ecology and*

594   *Systematics* 4: 1-23.

595 I.N.G.V. (2013). "The National Institute of Geophysics and Vulcanology." http://www.ingv.it/en/.

596 Jalal, M. M. (2008). "Performance Measurement of Water Distribution Systems (WDS) - A critical and

597   constructive appraisal of the state-of-the-art," *Master of Applied Science*, University of Toronto,

598   Toronto.

599 Jayaram, N., and Srinivasan, K. (2008). "Performance-based optimal design and rehabilitation of water

600   distribution networks using life cycle costing." *Water Resources Research*, 44(1), W01417.

601 Javanbarg, M.B., Scawthorn, C. and Takada, S. (2008). Priority evaluation of seismic mitigation in

602   pipeline networks using multicriteria analysis fuzzy AHP. *14th World Conference on Earthquake*

603   *Engineering*.

604 Kim, Y., Song, J., Spencer, B. and Elnashai, A. S. (2010). Seismic risk assessment of complex
605   interacting infrastructures using matrix-based system reliability method. *Tenth International*
606   *Conference on Structural Safety & Reliability.* 2889-2893.

607 Markov, I., Grigoriu, M., and O'Rourke, T. D. (1994). "An Evaluation of Seismic Serviceability Water
608   Supply Networks with Application to the San Francisco Auxiliary Water Supply System."
609   *Technical Report NCEER-94-0001*. Multidisciplinary Center for Earthquake Engineering
610   Research, Buffalo, NY.

611 Miles SB, Chang SE. "Modeling community recovery from earthquakes." *Earthquake Spectra*
612   *2006;22(2):439–58*

613 Mileti, D. (1999). *Disasters by Design: A Reassessment of Natural Hazards in the United States*, Joseph
614   Henry Press (May 18, 1999) Washington D.C.

615 Miller-Hooks, E., Zhang, X., and Faturechi, R. (2012). "Measuring and maximizing resilience of freight
616   transportation networks." *Computers & Operations Research*, 39(7), 1633-1643.

617 Ouyang, M., and Duenas-Osorio, L. (2011). "An approach to design interface topologies across
618   interdependent urban infrastructure systems." *Reliability Engineering & System Safety*, 96(11),
619   1462-1473.

620 Ouyang, M. (2014). "Review on modeling and simulation of interdependent critical infrastructure
621   systems." *Reliability engineering & System safety*, 121, 43-60.

622 Panza, G. F., Mura, C. L., Peresan, A., Romanelli, F., and Vaccari, F. (2012). "Seismic Hazard
623   Scenarios as Preventive Tools for a Disaster Resilient Society." *Advances in Geophysics*, 53, 93-
624   165.

625   Panza, G. F., Peresan, A., and Magrin, A. (2014a). "Neo-deterministic seismic hazard scenarios for

626   Friuli Venezia Giulia and surrounding areas ", ISPRA- Istituto Superiore per la Protezione e la

627   Ricerca Ambientale - Servizio Geologico d'Italia.

628   Panza G.F., Kossobokov V., Peresan A., Nekrasova A. (2014b). Chapter 12." Why are the standard

629   probabilistic methods of estimating seismic hazard and risks too often wrong?". In: Wyss M,

630   Shroder J (eds) Earthquake Hazard, Risk, and Disasters. Elsevier, London, 309-357.

631   Park, J., Seager, T. P., Rao, P., Convertino, M., and Linkov, I. (2013). "Integrating risk and resilience

632   approaches to catastrophe management in engineering systems." *Risk Analysis*, 33(3), 356-67.

633   Prasad, T. D., and Park, N.-S. (2004). "Multiobjective genetic algorithms for design of water distribution

634   networks." *Journal of Water Resource Planning and Management, ASCE*, 130(1), 73-82.

635   Queiroz, C., Garg, S. K., and Tari, Z. (2013). "A probabilistic model for quantifying the resilience of

636   networked systems." *Ibm Journal of Research and Development*, 57(5).

637   Rossman, L. A. (2000). "EPANET users manual." *EPA/600/R-00/057*, National Risk Management

638   Research Laboratory, Cincinnati, OH 45268.

639   Sabetta, F., and Pugliese., A. (1987). "Attenuation of peak horizontal acceleration and velocity from

640   italian strong-motion records." *Bulletin of the Seismological Society of America*, 77(5), 1491-1513.

641   Shinozuka, M., Hwang, H., and Murata, M. (1992). "Impact on Water Supply of a Seismically Damaged

642   Water Delivery System." *Lifeline Earthquake Engineering in the Central and Eastern US,*

643   *Technical Council on Lifeline Earthquake Engineering Monograph No.5.* Ballantyne, D. B., ed.,

644   ASCE, Reston, VA, 43-57.

645   Tamvakis, P., and Xenidis, Y. (2013). "Comparative Evaluation of Resilience Quantification Methods

646   for Infrastructure Systems." *Selected Papers from the 26th Ipma (International Project*

647   *Management Association), World Congress*, 74, 339-348.

648   Taylor, C. E. (1991). "Seismic Loss Estimation for a Hypothetical Water System." *Technical Council on*

649   *Lifeline Earthquake Engineering Monograph No.2*. ASCE, Reston, VA.

650   Tinebra, A. (2013). "Resilience Based Design of an Urban Water Distribution System " Master of

651   Science Thesis, Politecnico di Torino, Turin.

652   Todini, E. (2000). "Looped water distribution design using a resilience index based heuristic approach."

653   *Urban Water*, 2(2), 115-122.

654   Wang, Y., and O'Rourke, T. D. (2008). "Seismic Performance Evaluation of Water Supply Systems."

655   *Technical Report MCEER-08-0015*, The Multidisciplinary Center for Earthquake Engineering

656   Research (MCEER), Buffalo, NY.

657

LIST OF TABLES

670

671   Table 1-Charateristics of the pressure Reducing Valves

Id. code	Location	D (mm)	Meters Head (m)
PRV1	Via Dranza	63	20.0
PRV2	Via Giudea	63	15.0
PRV3	Via Vita	63	20.0
PRV4	Via Roma	110	20.0
PRV5	Via Maddalena II	110	15.0
PRV6	Via Teatro	63	25.0
PRV7	Via Maddalena II	110	20.0

672
673

674

675 Table 2- Scenarios considered in the analysis

Scenario	District Location & Group	Location	D (mm)	Average Flow loss (l/s)
1	S1_Main Pipeline	Break of DN 160 PE pipe in Via Conte Ruggero	160	90.11
2	S2_District 1	Break of DN 160 PE pipe in Matrice Square	160	180
3	S2_District 2	Break of DN 63 PE pipe in Via Giudea	63	61.4
4	S2_District 3	Break of DN 63 PE pipe in Via Vita	63	48.63
5	S2_District 4	Break of DN 63 PE pipe in Via Nazionale SS 290	63	53.80
6	S2_District 5	Break of DN 110 PE pipe in Via Nazionale SS 290	110	77.35
7	S2_District 6	Break of DN 63 PE pipe in Via Teatro	63	53.82
8	S2_District 7	Break of DN 110 PE pipe in Via Maddalena II	110	48.36
9	S2_District 8	Break of DN 110 PE pipe in Via Nazionale SS 290	110	75
10	S3_District 1	Break of DN 63 PE pipe in Via Itria	63	33.48
11	S3_District 2	Break of DN 110 PE pipe in Via Giudea	110	66.61
12	S3_District 3	Break of DN 63 PE pipe in Via Minavento	63	21.51
13	S3_District 4	Break of DN 63 PE pipe in Via San Antonio	63	24.47
14	S3_District 5	Break of DN 110 PE pipe in Via Maddalena II	110	55.25
15	S3_District 6	Break of DN 63 PE pipe in Via Annunziata	63	29.55
16	S3_District 7	Break of DN 110 PE pipe in Via Maddalena II	110	38.78
17	S3_District 8	Break of DN 110 PE pipe in Via Nazionale SS 290	110	44.54
18	S4_D1-D2	Break of DN 63 PE pipe in Umberto Square	63	58.05
19	S4_D2-D6 (I)	Break of DN 110 PE pipe in Via Roma	110	71.75
20	S4_D2-D6 (II)	Break of DN 110 PE pipe in Via Roma	110	70.29
21	S4_D2-MP	Break of DN 110 PE pipe in Via Nazionale SS 290	110	87.59
22	S4_D3-D6 (I)	Break of DN 63 PE pipe in Via Fontana	63	33.01
23	S4_D3-D6 (II)	Break of DN 63 PE pipe in Via Aquila	63	33.29
24	S4_D3-D8 (I)	Break of DN 63 PE pipe in Via Scarlata	63	31.72
25	S4_D3-D8 (II)	Break of DN 63 PE pipe in Via Scarlata	63	28.49
26	S4_D4-D5	Break of DN 110 PE pipe in Via Chiusa	110	63
27	S4_D4-D8	Break of DN 63 PE pipe in Via Lucchese	63	27.94
28	S4_D6-MP	Break of DN 160 PE pipe in Umberto Square	160	78.04
29	S1_MainPipeline	Braek of DN 110 PE pipe in Via P.D'Aragona	110	4.28

676
677
678

679

680 Table 3- Resilience Index summary for different scenario events

Scenario	R_1	R_2	$R=R_1×R_2$	Scenario	R_1	R_2	$R=R_1×R_2$	Scenario	R_1	R_2	$R=R_1×R_2$
1	0.40	0.69	0.28	11	0.92	0.19	0.18	20	0.86	0.23	0.20
2	0.79	0.88	0.69	12	0.95	0.74	0.71	21	0.58	0.64	0.37
3	0.92	0.23	0.21	13	0.83	0.83	0.68	22	0.84	0.64	0.54
4	0.95	0.31	0.29	14	0.93	0.45	0.42	23	0.84	0.64	0.54
5	0.82	0.34	0.28	15	0.89	0.91	0.81	24	0.93	0.60	0.56
6	0.90	0.33	0.30	16	0.97	0.56	0.54	25	0.94	0.64	0.60
7	0.88	0.31	0.28	17	0.92	0.41	0.37	26	0.85	0.36	0.30
8	0.97	0.38	0.37	18	0.88	0.57	0.5	27	0.96	0.65	0.62
9	0.87	0.11	0.10	19	0.86	0.23	0.20	28	0.42	0.69	0.29
10	0.90	0.59	0.53					29	0.78	0.36	0.28

681

682

683

684

685

686

687

689 LIST OF FIGURES

712

713

Figure1

715

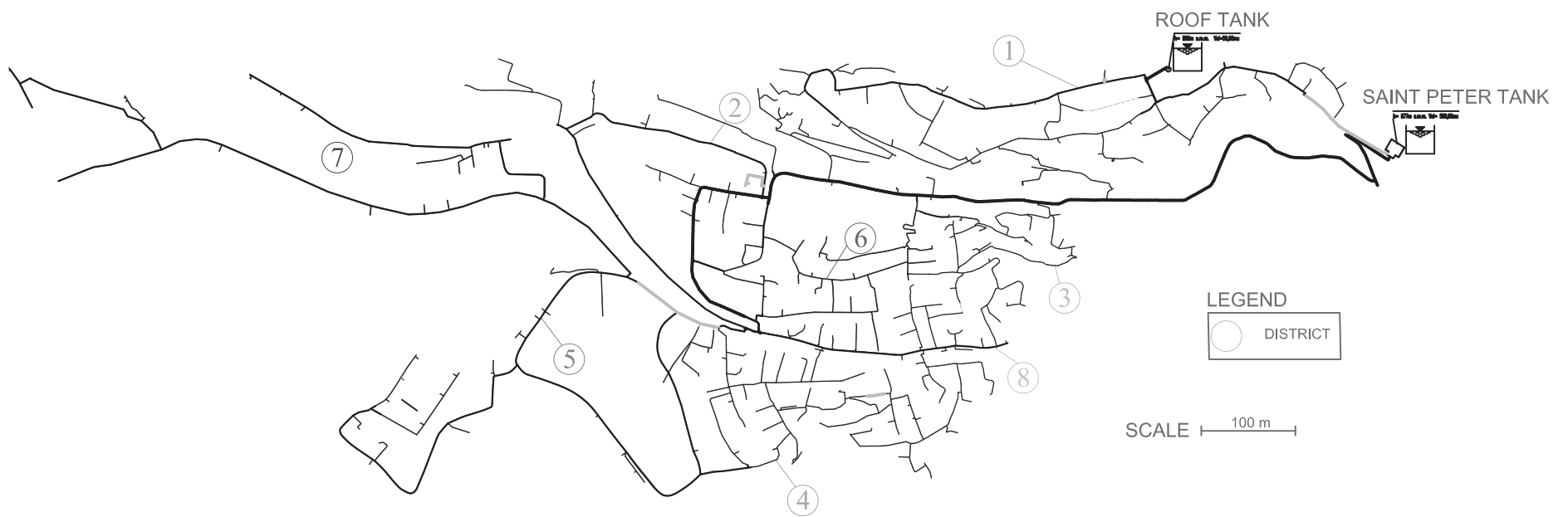716   (a)   (b)

717   Figure 1-(a) Functionality of Water Distribution System based on the number of users with suffered
718   water outage and of (b) the tank water height $F_z(t)=h(t)/h_{reserve}$. $IR_{ES,1}$ and $IR_{ES,2}$ represent the area under
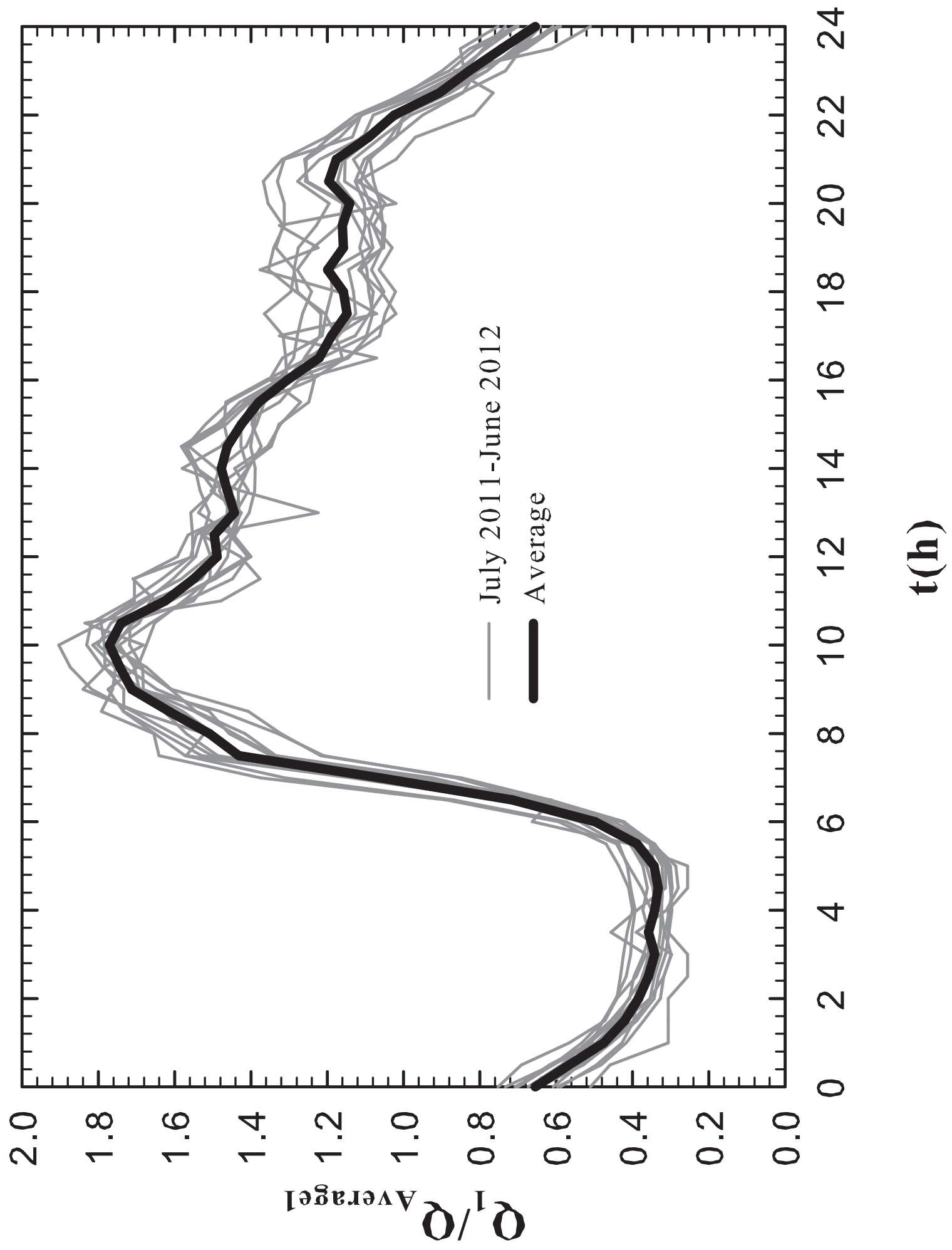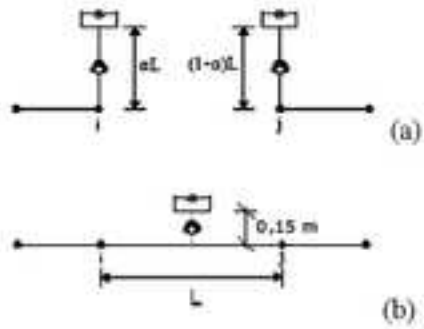719   the functionality curves.

720

Figure2

721
722
723   Figure 2–Location and overview of Calascibetta Town in Sicily
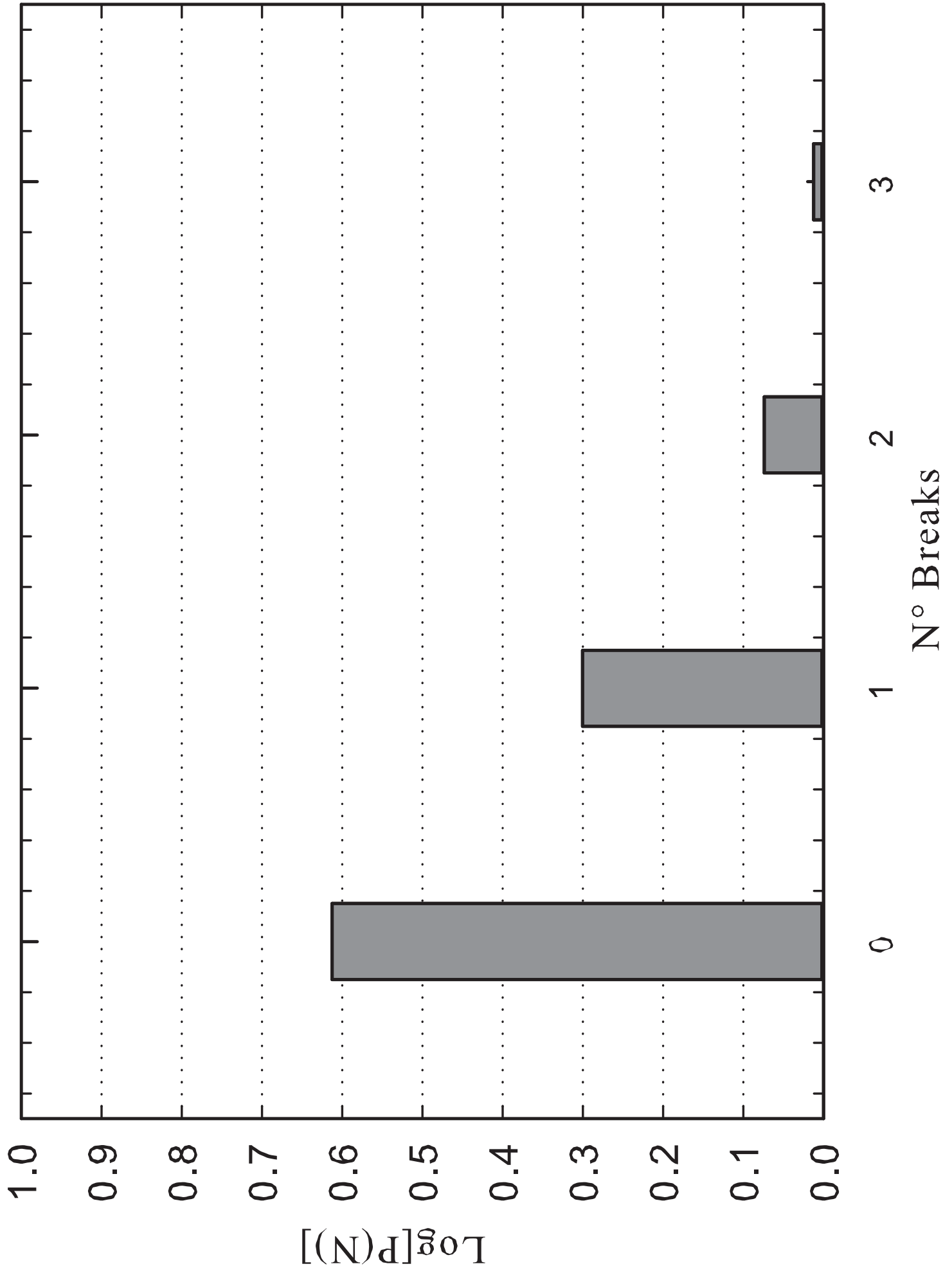
724

Figure4

Figure4

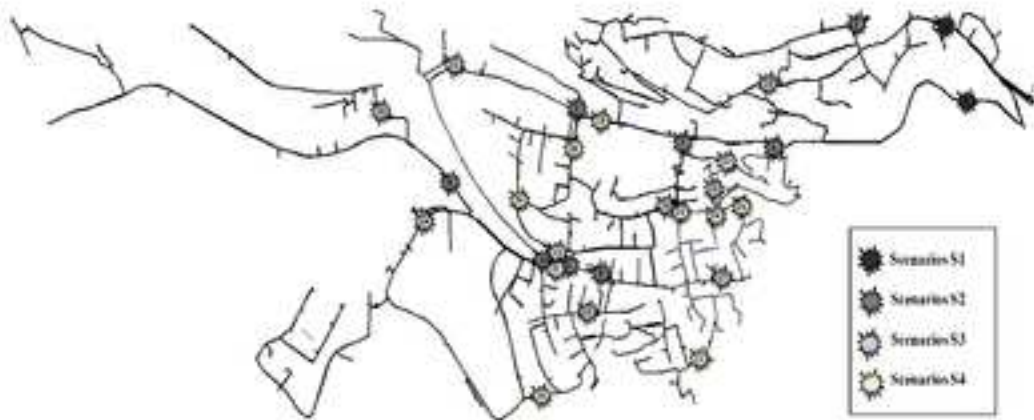739   Figure 5–Modeling of (a) Pipe Break Simulation and

740   (b) Pipe Leak Simulation in EPANET 2.0 (GIRAFFE, 2008)
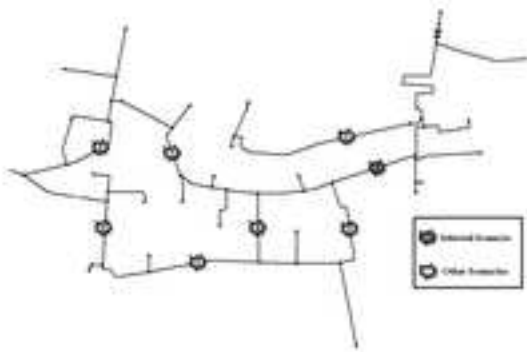
741

742

Figure6

Figure7

748

749

750   Figure 7-Earthquake Scenarios Event divided by groups

751

Figure8

752

753   Figure 8- Scenarios in District 6 for group S3

754

755

756

Figure9

Figure10

Figure11

Figure12

Figure12

Figure13

Figure14

Figure14

Figure15